WIND FLOWS AND FORCES IN A MODEL SPRUCE FOREST

G. R. STACEY, R. E. BELCHER, C. J. WOOD
Department of Engineering Science, Oxford University U.K.

and

B. A. GARDINER
Forestry Commission, Northern Research Station, Roslin, Midlothian, U.K.

(Received in final form 4 November, 1993)

Abstract. Wind tunnel tests have been conducted on a 1:75 scale model of a Sitka spruce forest in a correctly scaled turbulent boundary-layer flow. 12000 tree models were manufactured with mass, flexibility and aerodynamic drag characteristics chosen to give dynamical similarity with typical 15 m trees in a 30 ms^{-1} gale. To measure the dynamic response of a sample tree, set within this model forest, a miniature, fast response strain-gauge balance was designed and built. Linked to a computer for on-line data sampling, this balance provided measurements of the fluctuating along-wind and across-wind components of the overturning moment at ground level, leading to values of mean and extreme moments and the frequency spectrum of the sway motion. Associated measurements of local wind flow characteristics were made with hot-wire anemometers and a laser anemometer. The response of the tree has the characteristics of classical lightly damped vibration and there is evidence that resonant sway motion increases the extreme overturning moments significantly above the values produced by wind gust forces alone.

1. Introduction

A major contribution to softwood timber supplies in Europe is made by plantation-grown Sitka spruce trees, often grown on poor soils in exposed upland areas. In the UK, planting is usually dense with approximately 3500 trees per hectare. This is equivalent to a spacing of 1.7 m between trees.

Sitka spruce are normally harvested when they reach a height of approximately 20 m. This is not the maximum for the species; neither is it the optimum height for quantity or quality of timber. It is an unfortunate fact that when trees on poor soil and in exposed locations are allowed to grow above this height, wind damage causes a disproportionately increasing loss of production. Therefore it is usually more economical to cut the trees down before there is significant risk that they will be blown down. Taking account of this premature harvesting, as well as actual destruction, wind damage in the E.E.C. countries causes severe financial losses.

Research to seek ways to alleviate these losses has been sponsored by the Commission of the European Communities. As part of this programme, the Oxford University Wind Engineering Research Group has undertaken an extensive study in collaboration with the U.K. Forestry Commission (Northern Research Station), Edinburgh. Measurements to determine the aeroelastic characteristics of a typical Sitka Spruce tree have been undertaken at a NRS site by Gardiner (1989)

Boundary-Layer Meteorology **69**: 311–334, 1994.

and in the first paper of the present series (Gardiner, 1994), the wind structure at this site is described, together with the proposition that coherent 'Honami' gusts may be the principal cause of damage.

This second paper now describes the design of 1:75 scale aeroelastic tree models for the wind tunnel experiment, the air flow over the model canopy and the response of the tree models in terms of mean and extreme overturning moments at ground level.

Others have tested tree models in wind tunnels. Meroney (1968) modelled the drag characteristics of several species and studied the wind flow in and above the canopy, but there was no attempt at aeroelastic modelling. More recently, Papesch (1984) filmed the dynamic response of tree models with a correctly scaled natural frequency. However, his wire-brush models were excessively heavy and stiff, and the dynamical similarity was incomplete. A realistic representation of both flexibilty and natural frequency was achieved by Finnigan and Mulhearn (1978), but the crop represented was wheat, and not trees.

The originality of the present experiments is twofold. Firstly there is an attempt to produce an aeroelastic model tree, correctly scaled according to the established rules of dynamical similarity, and secondly the models have been instrumented for the direct measurement of the fluctuating overturning moments.

2. Design of the Wind Tunnel Experiment

2.1 Modelling the Natural Wind

In the earlier experiments cited above, the models were exposed to flows with an arbitrary velocity profile and turbulence. For the present experiments in the 4 m × 2 m Oxford University boundary-layer tunnel, a turbulence-generating grid was fixed at the inlet and an array of blocks was laid on the floor of the 12 m flow development section. These devices controlled the wind velocity profiles and the associated gust amplitudes and frequencies.

The quality of the flow was judged by comparison with empirical data on full-scale wind. [Engineering Sciences Data Unit (ESDU International plc), 1989]. Two target flows were selected. The first was the flow over an infinite fetch of uniform tree-canopy roughness ($z_0 = 0.5$ m), and the second was the flow over uniform farmland, representing typical terrain upstream of a forest edge ($z_0 = 0.1$ m). In the ESDU correlation, z_0 defines not only the conventional intercept of the logarithmic mean velocity profile, but also a complete description of the turbulence structure. The target flows associated with each selected value of z_0 are compared in Figures 1, 2 and 3 with those achieved in the wind tunnel.

For this comparison, the model trees were not installed, and the flow was measured over the locally smooth tunnel floor. To match this, the target velocity and turbulence profiles were computed to include the local speed-up caused by a corresponding smooth fetch close to the measurement point. This procedure pro-

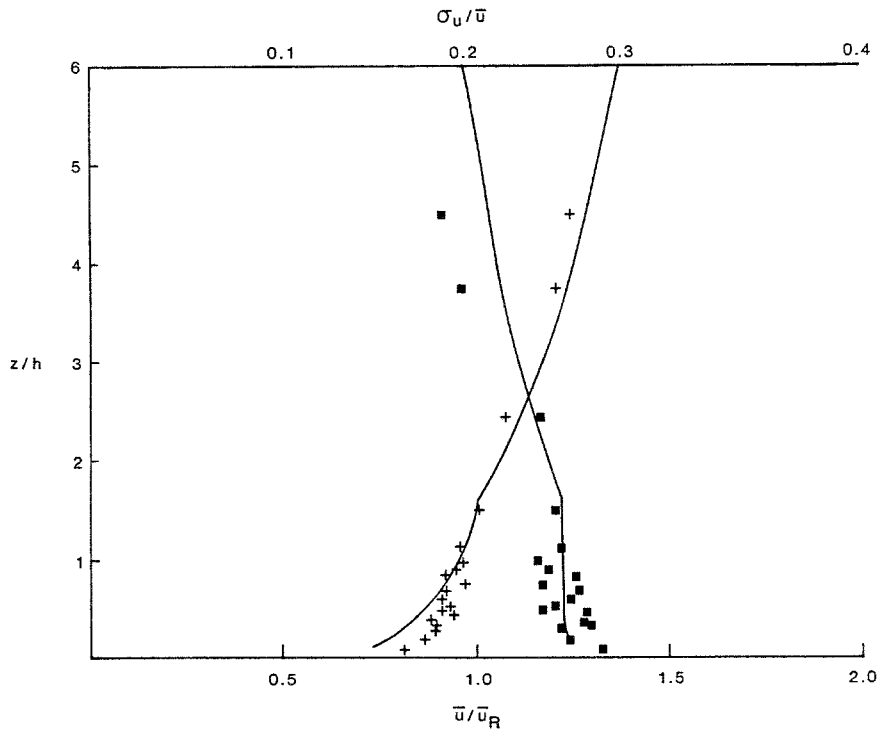

Fig. 1. Mid-forest simulation velocity (+) and turbulence intensity (*) profiles with ESDU target profiles.

vides a rigorously defined equivalence in the generalised flow conditions, before the installation of the tree models or the corresponding growth of full-scale trees. The agreement is good, including the kink in the profiles.

A comparison of gust frequencies is shown in Figure 3. Frequencies in the wind tunnel are related to full-scale frequencies by the requirement that the Strouhal Number (Frequency × Size/Wind speed) shall be the same in both cases (See Section 2.3). The difference between the two target flows is small and in Figure 3, only one comparison is shown.

2.2 The plantation model

The model plantation contained 12000 flexible model trees. The development was done in Edinburgh by Gardiner, with testing in the Oxford wind tunnel. For the final production, the stems were injection-moulded in Nylon-66, and over these were fitted sets of idealised branch elements, moulded in Low Density Polyethelyne. These produced approximately the correct overall shape and aerodynamic drag. Figure 4 shows some trees mounted on the balance.

To represent variations in growth, one third of the models were made 200 mm tall, to represent 15 m trees at the chosen scale of 1:75, one third were 210 mm

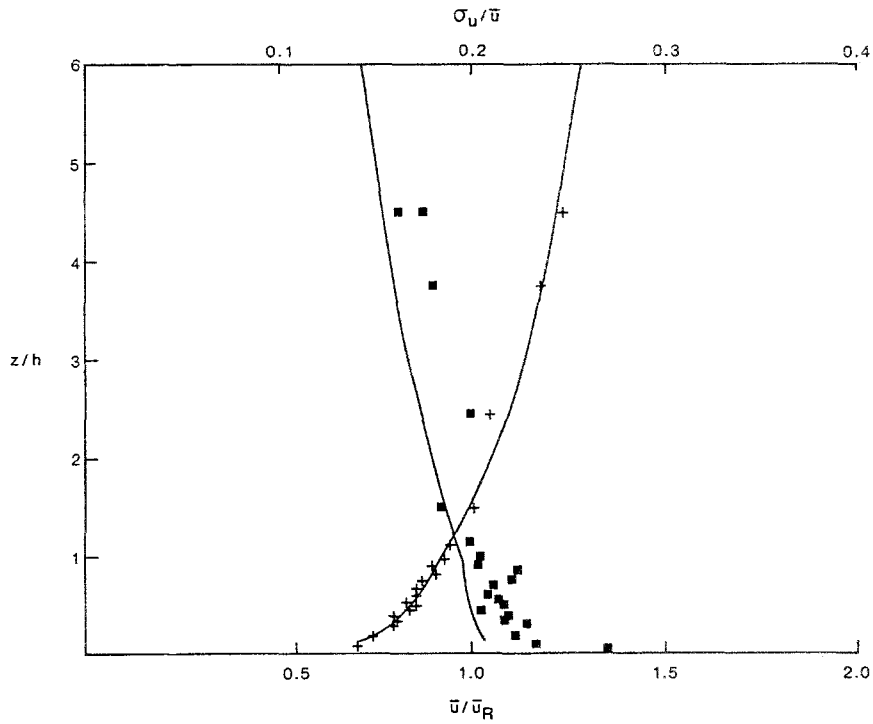

Fig. 2. Forest edge simulation velocity (+) and turbulence intensity (*) profiles with ESDU target profiles.

tall, and one third were 190 mm. The three sizes were randomly inserted in pre-drilled panels, covering a 2.4 m square area of the wind tunnel floor. The basic spacing was 23.1 mm (1.73 m full scale). Thinned patterns and special arrangements are discussed in the third paper of this series (Gardiner *et al.*, 1994).

2.3 Design of the aeroelastic tree models

As in the design of the wind tunnel flow, so in the design of aeroelastic model trees, it is necessary to observe the requirements for dynamical similarity. This is a routine technique [e.g., Massey 1983], and it will not be described here. Table I defines a list of 12 variables characterising the wind flow and the aerodynamic and elastic properties of the tree, including the still-air damping ratio ζ. This latter parameter controls the ratio $e^{-\delta}$ of successive peak sway deflections in still air, through the definition ($\delta = 2\pi\zeta/(1 - \zeta^2)$).

This list is necessarily simplified. For example, the natural sway frequency is taken to be the frequency of the first bending mode; and higher modes were not examined. Also, the aerodynamic features of the tree are simplified by regarding the tree as a lumped system which obstructs the local airflow and causes a drag D, acting at the centre of pressure. Accepting these simplifications, Table II is

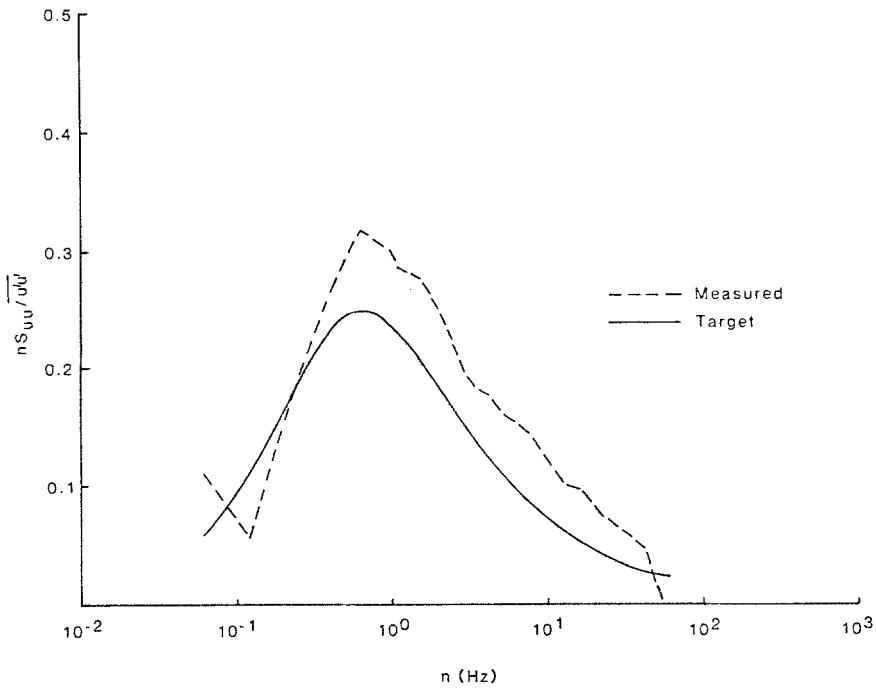

Fig. 3. Target and actual mid-forest wind spectra.

generated from Table I by dimensional analysis, and contains 9 dimensionless parameters. These relate the design of the 1:75 scale tree models at a nominal tunnel speed of 6 m/s, to a typical 15 m Sitka Spruce in a 30 ms^{-1} gale. The full-scale data is from Gardiner (1989).

2.4 Assessment of dynamical similarity

In Table II, eight of the dimensionless parameters represent experimental conditions that are controlled independently. The ninth is the uprooting- or base-bending moment coefficient which is the desired result of the experiment. For complete dynamical similarity, each of the independent parameters should have the same values for the model as at full-scale. If this condition is satisfied, then the bending moment coefficients will also be equal. Full-scale bending moments are then calculated from corresponding wind tunnel moment coefficients, simply by using appropriate full-scale values for the air density ρ, the tree height H and the reference mean wind speed $\bar{u}_R$, measured at 28.5 m above ground or 380 mm in the wind tunnel.

Examining the full-scale and model values in Table II, it is obvious that the wind structure modelling is good, and the frequency and damping of the trees are correctly represented. However, in the case of the dimensionless mass, the equality

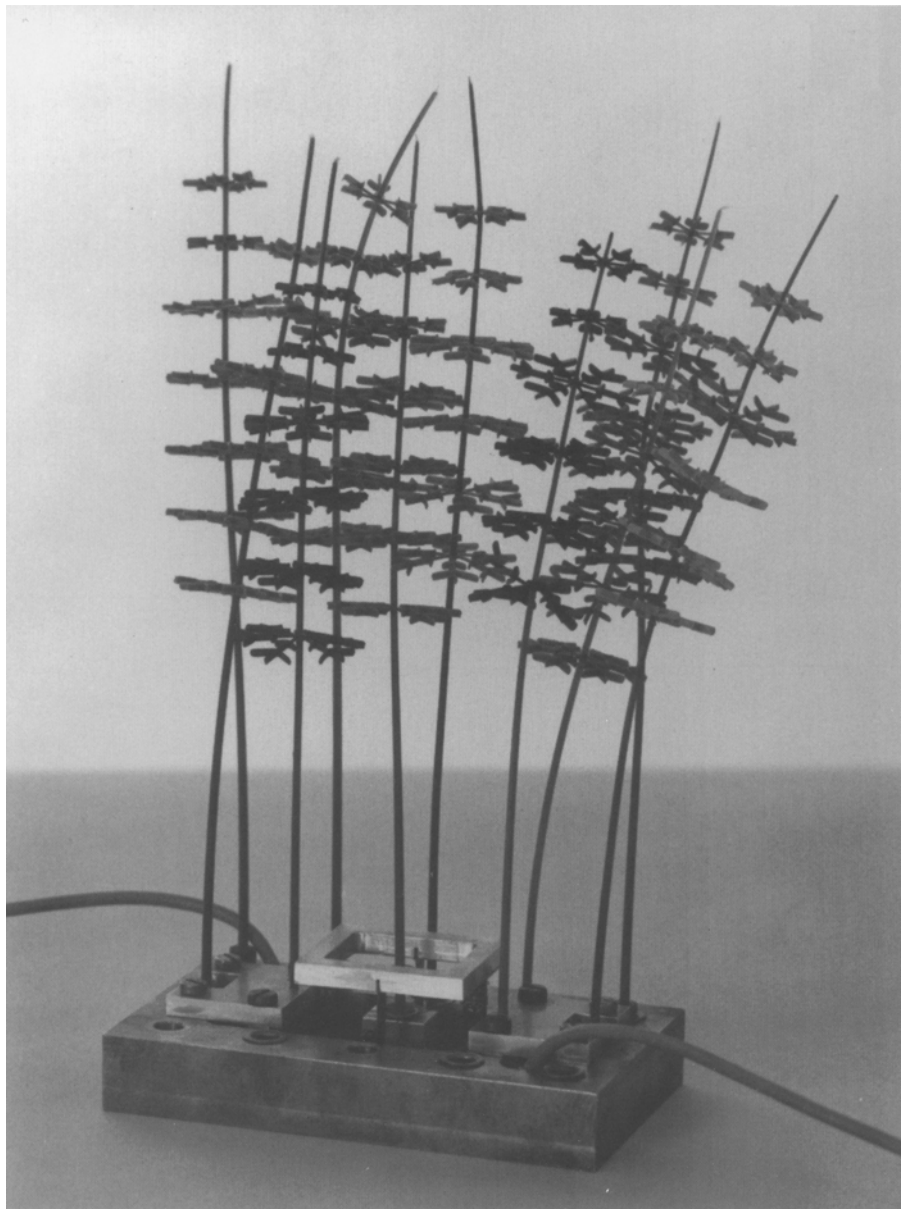

Fig. 4. Model trees on bending moment balance.

condition has not been satisfied so well. Also, as in all small-scale experiments, the Reynolds number is in error. Finally, the representation of the drag coefficient is uncertain. Therefore dynamical similarity is not complete, and a reason must be stated for believing that these three modelling errors will not destroy the equality of the model and full-scale bending moment coefficients.

TABLE I

List of parameters characterising wind induced motion of flexible trees

Name of variable	Symbol	Full scale value	Model value
Description of Tree			
Height of individual tree (m)	H	15	0.2
Nominal canopy height (m) for Figures	h	15	0.2
Total mass (kg)	M	211.8	1.04×10^{-3}
(Live branch mass for Equations (1) and (2) (kg))	(m)	(49.5)	(0.64×10^{-3})
Natural sway frequency (Hz)	f	0.33	4.9
Still-air damping ratio	ζ	0.048	0.048
Drag force in uniform flow test (Newtons)	D	Equation (1)	Table II
Description of the wind			
Reference mean wind speed at 28.5 m (ms^{-1})	$\bar{u}_R$	30	6
Mean wind velocity profile (ms^{-1})	$\bar{u}$	Figures 1, 2, 5	Figures 1, 2, 5
Gust standard deviation profile (ms^{-1})	σ_u	Figures 1, 2, 6	Figures 1, 2, 6
Gust frequency at stated height (Hz)	n	Figure 3	Figure 3
Nominal air density ($kg\,m^3$)	ρ	1.225	1.225
Nominal air viscosity ($kg\,m^{-1}\,s^{-1}$)	μ	1.8×10^{-5}	1.8×10^{-5}
Result of experiment			
Fluctuating bending moment at base of tree	Q	**	**

** Dependent variables, arising as results of the experiment.

TABLE II

List of dimensionless parameters

Name of parameter	Symbol	Full scale value	Model value
Tree Characteristics			
Mass	$M/\rho H^3$	0.051	0.102
Natural sway frequency	$fH/\bar{u}_R$	0.165	0.163
Still-air damping ratio	ζ	0.048	0.048
Drag coefficient in uniform flow at speed U	$D/(\frac{1}{2}\rho U^2 H^2)$	Equation (2)	0.018
Description of the wind			
Mean wind speed ratio at stated height	$\bar{u}/\bar{u}_R$	Figures 1, 2, 5	Figures 1, 2, 5
Turbulence intensity at stated height	$\sigma_u/\bar{u}$	Figures 1, 2, 6	Figures 1, 2, 6
Gust frequency at stated height	$nH/\bar{u}$	Figure 3	Figure 3
Nominal Reynolds number	$\rho\bar{u}_R H/\mu$	3.1×10^7	8.2×10^4
Result of experiment			
Bending moment coefficient at base of tree	$Q/(\frac{1}{2}\rho\bar{u}_r^2 H^3)$	**	**

** Values at model scale and at full-scale should be equal.

2.4.1 *Mass and Stiffness*

In the experimental development of the tree models, the excessive mass has been offset by a correspondingly increased bending stiffness, to give the correct natural sway frequency f. When considered together with the well-matched damping ratio ζ, this means that the first mode free vibration of the trees will be correctly reproduced at any reasonable amplitude. However, simple theory of vibrations

indicates that the displacement amplitude is proportional to the ratio of the exciting force to the mass. Consequently the excessive stiffness of the tree models means that, for a given wind force excitation, the sway amplitudes will be too small by a factor 0.051/0.102. On the other hand, the ratio of the overturning moment Q to the exciting force D at any frequency is a function only of the natural frequency f and the damping ratio ζ. Therefore the bending moment measurements will be correct even though the sway amplitudes are not.

It might be thought that the insufficient sway amplitude of the present models would lead to an underestimate of the moment contribution due to overhanging weight. However, because the reduced sway amplitude is accompanied by a proportionally increased weight, this contribution remains correct also.

There are two secondary consequences of the reduced sway of the tree models. Firstly it is not certain whether the error decreases any feedback to the local turbulence, and secondly there will be a reduction in crown clashing.

2.4.2 *Reynolds Number*

Normally, if the Reynolds number in an experiment is wrong, then the flow details and drag coefficient are probably wrong also. However, the mismatch is not a difficulty because the present experiment is designed specifically to sidestep the problem. Thus the tree models have been made realistic by designing the branches to give the desired drag coefficient despite the peculiar appearance. In the same way, the mean velocity and turbulence intensity profiles, and the gust frequencies in the onset flow have been made correct, not by relying on dynamical similarity, but by introducing artificial obstructions to generate the desired characteristics.

This procedure guarantees only those characteristics that are measured, however. There is no automatic justification for supposing that others (e.g., the higher probability moments that describe the intermittent and skewed nature of the gusts) will naturally be correct.

2.4.3 *A Problem with the Drag Coefficient*

The point of greatest uncertainty in the design of the tree models is the target value of the drag coefficient. The full-scale drag was not measured by Gardiner in the 1989 survey. Instead, use is made here of an empirical formula by Mayhead *et al.* (1975). This gives the drag D of an isolated Sitka spruce tree, in terms of the live branch mass m (kg) and the onset wind speed U (ms^{-1}). When corrected to give D in Newtons rather than kg, this becomes

$$D = 0.4352U^2 m^{0.667} \exp\{-0.0009779U^2\}. \tag{1}$$

It should be noted that the Mayhead measurements were in uniform flow. Thus in the present experiments, the aim has been to produce model trees with drag coefficients in agreement with Equation (1), when they also are tested in uniform flow. To make use of Equation (1), it must be written in dimensionless form to

yield a drag coefficient, as defined as in Table II. Substituting values of m, H and ρ from Table I yields the following expression, applicable to a typical 15 m tree.

$$C_D = 0.04257 \exp\{-0.0009779 U^2\} . \quad (2)$$

In this equation, C_D decreases with increasing wind speed, due to the streamlining effect of the branches bending in the wind. Unfortunately, it has proved impossible to manufacture tree models whose branches deflect to reduce the drag coefficient. The drag coefficient for the present tree models is 0.018, a value which, according to Equation (2), corresponds to the chosen nominal speed of 30 ms^{-1} (Table I).

It might be argued that the models should have been designed with the higher drag coefficient appropriate to the lower mean speeds within the canopy. On the other hand, damaging wind forces arise when the canopy is penetrated by an extreme gust, and measurements during the present wind tunnel programme have indicated that the gust speed at 80% tree height is frequently greater than $0.85\bar{u}_R$ (25 ms^{-1}) and occasionally greater than $1.05\bar{u}_R$ (31 ms^{-1}). Mayhead *et al.* do not provide information on the vertical distribution of the drag. The present models have been designed arbitrarily to give a centre of pressure in uniform flow, at approximately 80% tree height.

3. Experimental Method

3.1. Velocity measurements by hot-wire anemometer

Most of the wind tunnel measurements of the fluctuating longitudinal velocity $(\bar{u} + u')$ were made using a DANTEC single component linearised constant-temperature hot-wire anemometer, mounted on a robot traversing arm. The position sequence of the anemometer probe, and the sampling and analysis of the signal, were computer controlled, using programmes designed, and used regularly, by the Wind Engineering Research Group.

After pre-calibrating the anemometer to prove linearity of response, the mean velocity $\bar{u}$ and turbulence standard deviation $\overline{u'^2}$ were measured at selected locations, by sampling the anemometer signal at 10 ms intervals for up to 120 s, and performing the appropriate calculations on the data samples recorded. To measure gust frequency spectra, and the probability function for extreme gusts, similarly appropriate data sampling and analysis routines were used. All local anemometer measurements were related to a tunnel speed reference, by including in each automated sequence, a measurement adjacent to a pitot-static tube giving the dynamic pressure at a fixed tunnel reference location, well away from the model.

3.2. Wind speed measurements by laser anemometer

When used very close to the tree canopy, hot-wire anemometer probes are exceptionally vulnerable to mechanical damage by contact with the models. Also, in the highly turbulent flows at this level, the response of a hot wire anemometer is

inadequate. This is partly because the vertical hot-wire responds to the resultant velocity $\sqrt{(\bar{u} + u')^2 + v^2}$, which approximates the longitudinal velocity component $(\bar{u} + u')$ only when v is relatively small. A quite separate error arises if the mean velocity $\bar{u}$ is small and $(\bar{u} + u')$ ever becomes negative momentarily. The hot-wire, being a heat transfer detector, cannot distinguish negative velocities, and thus effectively rectifies the signal, causing errors in the mean and deviation.

For measurements in these locations, a DANTEC two-component fibre-optics laser anemometer was used, with atomised glycerine seeding in the 0.5 μm size range. Particles of this size may be expected to follow turbulent velocity fluctuations within 0.6% at frequencies up to 100 Hz.

Provided that the randomly timed data are correctly interpreted, the laser anemometer requires no calibration and gives absolute measurements of $(\bar{u} + u')$ and v' independently within a focus volume approximately 1.5mm long and 0.12 mm in diameter. A comparison of the two instruments showed good agreement between values of the mean velocity $\bar{u}$ above the canopy but, below tree height in the clearings, the hot-wire value of the resultant $\sqrt{(\bar{u} + u')^2 + v^2}$ was approximately twice the laser value of $\bar{u}$.

3.3. Measurement of ground-level bending moment

The miniature two-component balance shown in Figure 4 was constructed to measure simultaneously the fluctuating along-wind and across-wind components of the bending moment Q, at the base of a single tree model. Flexure strips carrying strain gauges were arranged in pairs to form hinges about the two horizontal axes in the ground plane, and the gauges were connected to two channels of a Welwyn strain gauge bridge. The sensitivity was 0.014 Nm per V, over a range of ± 0.03 Nm. Spectral analysis of the vibration response confirmed that the balance elements were very stiff compared with the flexible tree models. This ensured that the natural vibration of the models was not distorted when the models were mounted on the balance.

The balance module has plan dimensions 115.3 mm $\times$ 69.2 mm. This corresponds to a 5 $\times$ 3 array in the planting pattern, and the balance body itself carries 14 planting sockets, surrounding the single, central socket on the active balance element. Dummy modules, also 115 mm wide, and of various lengths, were provided, to complete the planting pattern along a strip between the separated main panels. By rearranging these, the balance module could be positioned anywhere within the array of trees.

Before each measurement sequence, the balance, together with the associated amplification and computer sampling system, was calibrated directly by inserting a rigid post in place of the tree model, and applying a sequence of horizontal loads at measured heights. After inserting the tree model, the zero was re-checked in the operating location in the wind tunnel.

A source of variability in the results was crown-contact with adjacent model trees, especially in the closely-spaced patterns. In the field trials, the damping

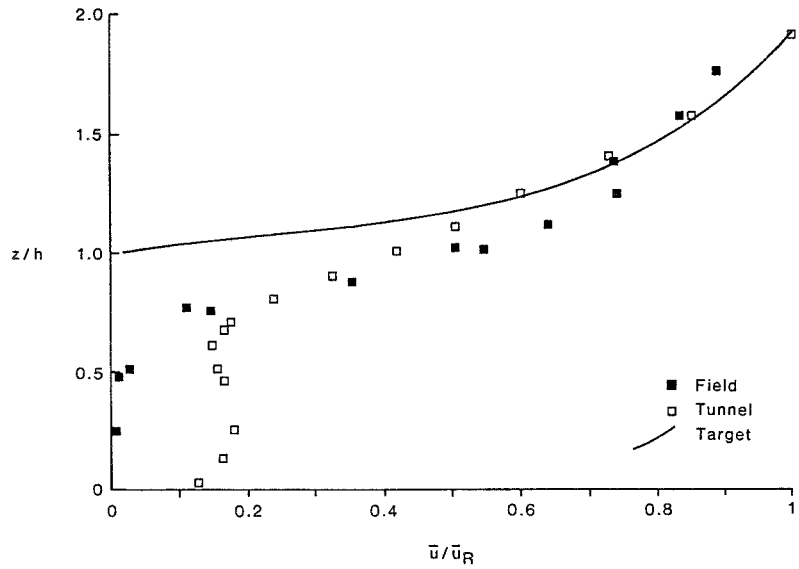

Fig. 5. Comparison of field, tunnel and target velocity profiles over mid-forest trees.

coefficient of 0.048 (Tables I and II), was found when adjacent trees were pulled aside to prevent clashing. When these were released to their normal positions, the apparent damping coefficient increased to 0.068.

On the model trees, the only damping coefficient measured was the value of 0.048, obtained from isolated models. Clashing between the Polyethelyne 'branches' caused more disruption than damping. This modelling error affects the most closely spaced tree patterns and is examined in more detail in the third paper of this series (Gardiner *et al.*, 1994).

4. Discussion of Mid-Forest Wind Structure

4.1. Velocity and turbulence profiles

The mid-forest (High z_0) wind simulation described in Section 2.1 was set up to match the ESDU target flow so that, when the plantation model was installed, the flow over the whole of the 2.4m square model area would correspond to the full-scale wind over an infinite uniform forest. Unfortunately, uniformity is not achieved immediately at the upstream edge of the model because the artificially simulated onset flow (Figure 1) has a ground-level origin, whereas the mid forest wind is effectively displaced to flow above the tree canopy. However, this transition is fairly localised, and over the centre of the model, the flow above the canopy shows good agreement with the ESDU target profiles (Figures 5 and 6). In this comparison, the target profiles are displaced arbitrarily to an origin at tree height

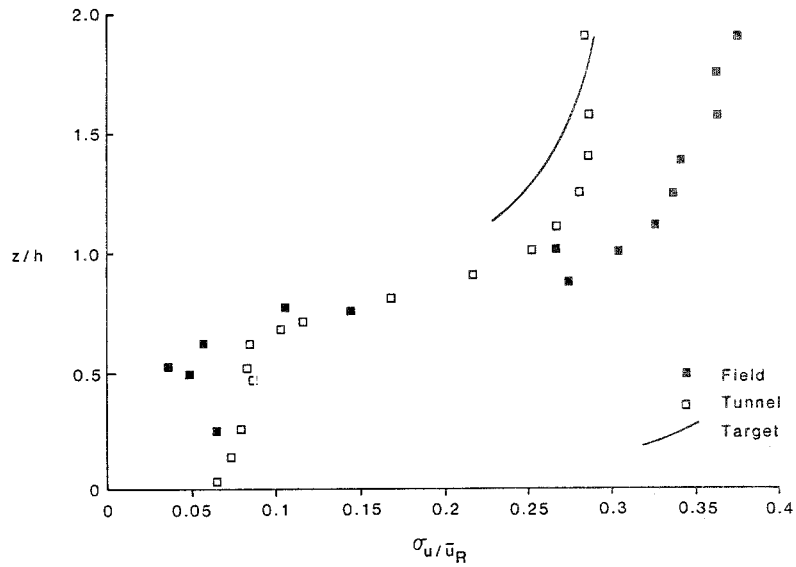

Fig. 6. Comparison of field, tunnel and target turbulence profiles over mid-forest trees.

(Lo, 1990) although a lower origin would have given equally reasonable agreement. Also included are corresponding data from the field measurements (Paper 1). Generally the agreement between the wind tunnel values and the average of the field results is encouraging, particularly in the top third of the canopy, which is of prime concern.

4.2. Effect of trees on gust frequency spectra

Figure 7 shows two tunnel gust frequency spectra, both measured at a height of 249 mm (1.25 h). The comparison is between frequencies above the plantation model centre and those at a location immediately upwind of the model. Both spectra are heavily smoothed to clarify the predominant differences, and the change suggests an increase in spectral energy near the 4.9 Hz tree frequency. This tendency is confirmed by similar measurements at other heights. Because the spectra were not recorded at the same location, it cannot be claimed that the differences are due exclusively to the tree motion. Nevertheless, the shift towards the tree sway frequency seems more than just a coincidence. The full-scale measurements in Paper 1, and reports of other investigators suggest a reduction of energy at tree frequency, but measured deep within the canopy rather than above it. In view of the lack of a rigorous experiment, the present authors are reluctant to draw firm conclusions at this stage, and the intriguing mechanism of energy exchange remains to be explored further.

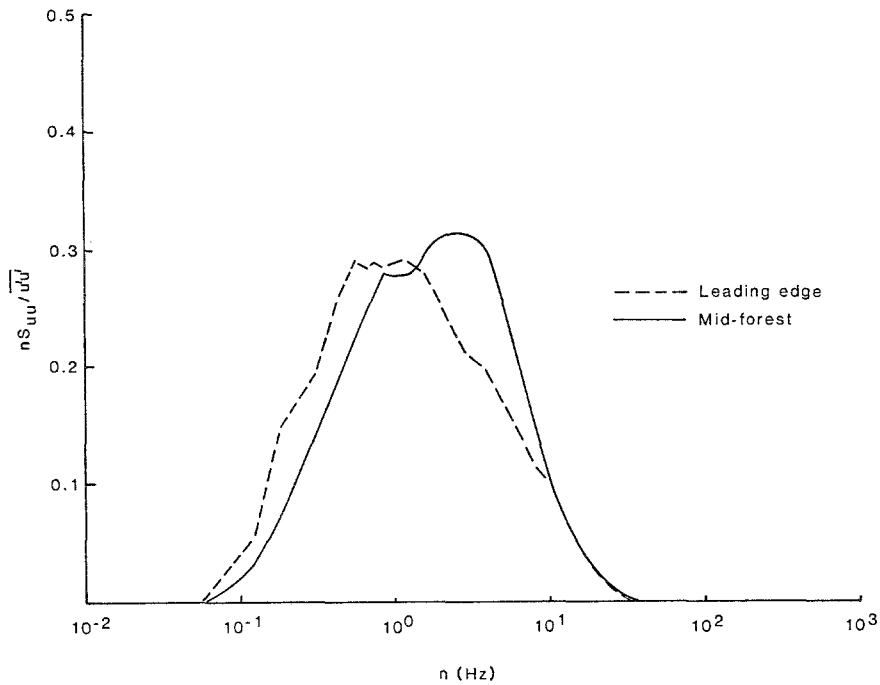

Fig. 7. Change in wind velocity spectrum due to trees at $z/h = 1.25$.

4.3. Extreme gust probability data

In addition to the velocity and turbulence profiles shown in Figures 5 and 6, extreme gusts were examined at three heights. To describe these, the Mode μ_u is defined from a probability distribution of the maximum 3-sec gust speed in an observation period of 10 min. The estimation procedure is that of Lieblein (1974, 1975). It uses 16 independent wind tunnel measurements of the largest gust in a continuous record of duration 40 s (equivalent to 10 min at full scale). Taking the ratio of the mode to the mean wind speed at the same point gives rise to a convenient Gust Ratio. Alternatively, a Gust Factor η may be defined to express the extreme excursion from the mean as a number of standard deviations (i.e., $(\mu_u - \bar{u})/\sigma_u$). The resulting values are shown in Table III.

The extreme value measurement was made at three heights only. To extrapolate the prediction to other heights, the mean velocity and standard deviation from the profile measurement (Figures 5 and 6) may be used with an estimated value of the gust factor η. This is done for $z/H = 0.8$ in the bottom row of Table III using a gust factor of 2.1, estimated by extrapolating the gust factor data in that column.

TABLE III

Mid-forest gust velocity ratios

Height z/h	Mean speed $\bar{u}/\overline{u_r}$	Std. dev. $\sigma_u/\bar{u}_R$	Mode $\mu_u/\bar{u}_R$	Gust factor η $(\mu_u - \bar{u})/\sigma_u)$	Gust ratio $\mu_u/\bar{u}$
1.90	1.000	0.291	1.52	1.79	1.52
1.57	0.839	0.311	1.47	2.03	1.74
1.25	0.599	0.294	1.21	2.08	2.01
0.8	0.241	0.168	No data Calc. 0.59	No data Est. 2.1	No data Calc. 2.46

5. Mid-Forest Bending Moments

5.1. Effect of wind direction

Using the balance described in Section 3.3, two components of bending moment could be measured on a single tree model, about orthogonal axes in the ground plane. With the balance mounted at the centre of the 2.4 m square model plantation, and aligned to detect along-row and cross-row moments, the whole model was rotated on the wind tunnel turntable, to vary the wind direction in 15° steps from 0° to 90°.

The two components were combined to give a resultant, approximately in the stream direction. The mean values were computed from samples at 10 ms intervals taken over 60 s, and the mode was obtained by the same procedure used for the extreme gusts (Section 4.3). The variate chosen to represent the extreme bending moment was the unfiltered instantaneous maximum moment, in a period of 40 s (equivalent to 10 min at full scale) and the mode of the associated probability distribution was again obtained by the procedure of Lieblein.

Using the coefficient definition from Table II, both mean and extreme bending moments are presented in Figure 8. Although there are some variations with wind direction, the random pattern of the changes suggests that these are not the result of any systematic directional effect, but are probably caused by differing tree interactions. Typical values are 0.0008 for the mean coefficients and ten times this value (0.008) for the corresponding 10-min modes.

In the field, direct measurements of uprooting moment have not been made, but extreme moment coefficients have been inferred from extreme sway deflections of three trees, calibrated by a pull-deflection method. The calibration of a tree as a self-transducer for uprooting moments is subject to a number of assumptions (Gardiner, 1994). Nevertheless the agreement with tunnel bending moments is too encouraging to be ignored. The estimates for the 3-s, 60 min mode obtained on three different days, are between 0.007 and 0.012.

6.2. Excitation mechanisms for extreme moments

As far as the authors are aware, this is the first time that measurements have been presented, showing the relationship between mean and extreme overturning

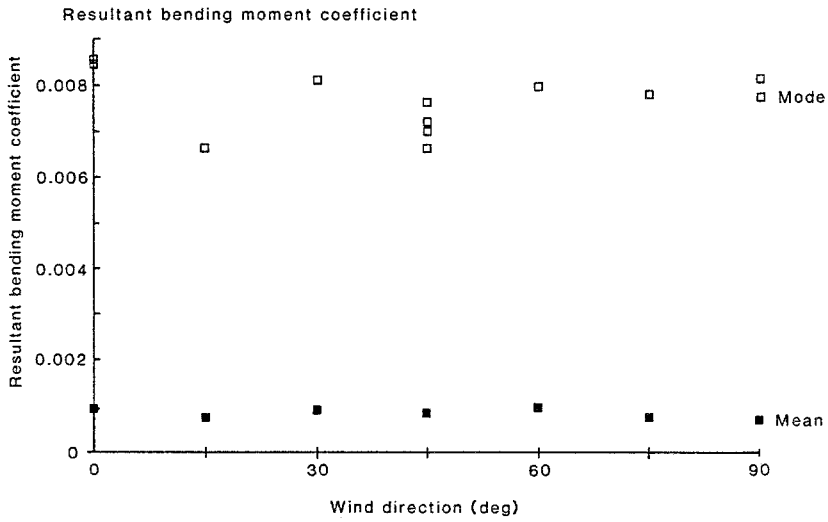

Fig. 8. Effect of wind direction on mid-forest bending moments.

moments on trees. In Figure 8, the extreme moments are shown to be nearly ten times the mean moments, and a key question is whether the mechanism driving these excursions is sway resonance or simply a quasi-steady response to gusts as they occur.

In the absence of comparative tests on elastic and non-elastic tree models, the problem may be considered by examining the sample bending moment spectrum in Figure 9c. This was measured simultaneously with the gust spectrum at 1.25 tree heights (Figure 9a). The ratio of these two spectra defines the tree sway response admittance function (Figure 9b). Figure 9b looks similar to that for the classical behaviour of a simple mass-spring-damper system, with unit amplification at low frequencies, a decay at very high frequencies and a predominant resonance in between. A similar conclusion has been drawn by Gardiner (1992) examining full scale sway displacements, and by Finnigan and Mulhearn (1978) for wheat.

Having identified this resonant behaviour, the assessment is completed by considering how the extreme values would be reduced if the resonant admittance function (Figure 9b) were replaced by a non-resonant constant factor, thus reducing Figure 9c to the dotted curve, directly proportional to Figure 9a. There are well known theoretical analyses, e.g., Cartwright and Longuet-Higgins (1956) and Davenport (1964), which establish relationships between spectrum shape and extreme values. These suggest that extreme values are increased by increasing the radius of gyration ν of the response spectrum (Figure 9c) about the zero-frequency axis, or in algebraic notation:

$$\nu^2 = \frac{\int n^2 S(n) d(\log_e(n))}{\int n S(n) d(\log_e(n))} \tag{3}$$

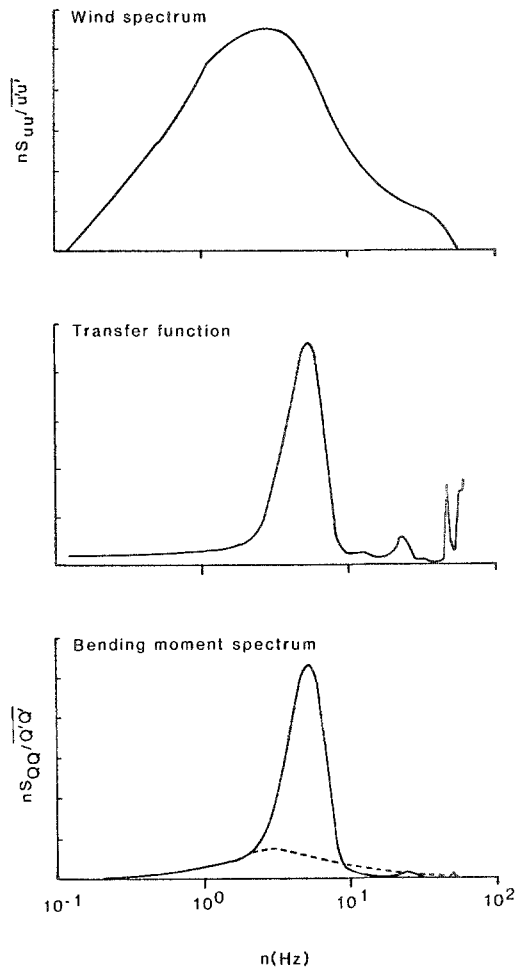

Fig. 9. Mid-forest wind and bending moment spectra with associated admittance function.

$$\eta = \sqrt{2 \log_e(\nu T)}\,, \tag{4}$$

where η = (mode − mean)/(standard deviation).

In Table IV, these equations are used to compare predicted extreme values for the measured bending moment spectrum in Figure 9c, and for the modified moment spectrum with the resonant response removed (Dotted curve in Figure 9c).

Equations (3) and (4) are unrealistic in that the theory assumes a Gaussian probability function. Nevertheless they provide a simple indication of the relationship between spectral information and extreme values. This allows us to conclude that resonance can be expected to increase significantly the extreme moment excursions (mode − mean). This effect is greatest when the tree resonant frequency is just to the right of the gust spectrum peak, but in Table IV, the

TABLE IV

Summary of extreme value estimation from spectra (normalised values)

	Wind at 1.25 H (Figure 9a)	Overturning moment coefficient (Figure 9c)	Estimated non-resonant moment coefficient
Mean	1.000	1.000	1.000
Standard deviation σ	0.491	0.885	0.429
(Mode–Mean)/σ(= η)	4.143	4.054	4.143
Mode–Mean	2.035	3.588	1.779
Mode	3.035	4.588	2.779

predominant effect is clearly the increase in the standard deviation caused by the resonance.

The assertion that resonance is important does not deny the physical reality of the Honami gusts discussed by Gardiner (1994). This phenomenon is clearly visible in the wind tunnel, taking the form of catspaw-like patches sweeping across the forest model. Also visible, and recorded on video tape, is the behaviour of the tree models within these 'Honami' patches. They do not simply lean to the gust, they wobble violently as it passes.

6. Effects at the Windward Edge of a Plantation

6.1. Wind profiles

Starting with the Open Farmland wind simulation (Figure 2), mean velocity and turbulence profiles were measured at six locations between 0.5 h upstream of the forest edge, and 9 h downstream. Figure 10 shows the mean wind speed variation by means of contours with an arbitrary velocity scale. This contour plot makes visible the progressive growth of a boundary layer above canopy height. Close above the canopy, mean speeds are reduced progressively with distance into the plantation. The cause of this is the tree drag which is equivalent on average, to a retarding shear stress. Near the upwind edge, this drag mechanism includes the deceleration of the air which enters the inter-tree space through the upwind edge of the plantation. Continuity ensures that some of this retarded air is expelled upwards, thus contributing to the wind speed deficit above the canopy. A second feature of Figure 10 is the dip in the contours above the leading edge of the plantation. This shows that the mean wind is accelerated locally, as would be expected over the upstream part of any obstruction. In corresponding locations, the standard deviation of the turbulent velocity fluctuations is reduced slightly (Figure 11).

More significant for gust loading on the trees is the fact that gust standard deviation increases in the region close above the canopy. Thus although the decay

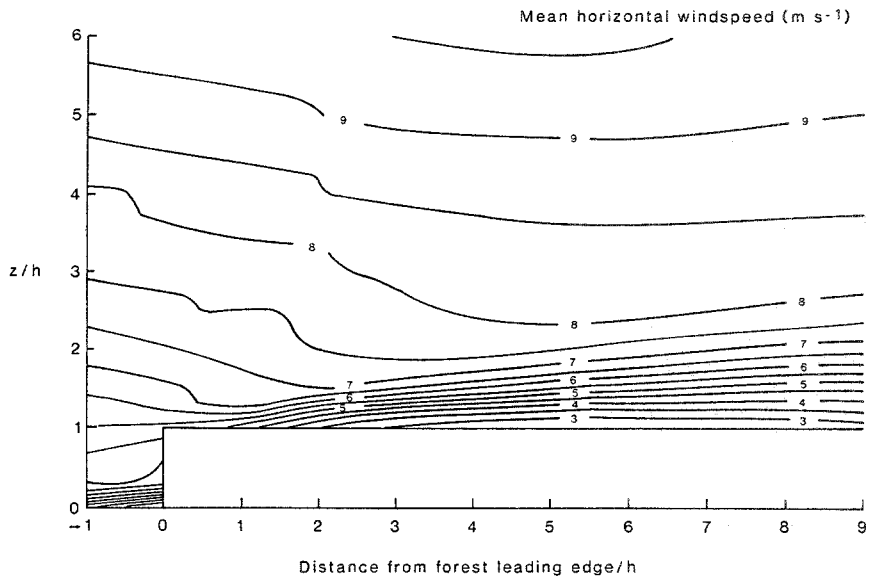

Fig. 10. Mean velocity contours at forest edge (Flow from left to right).

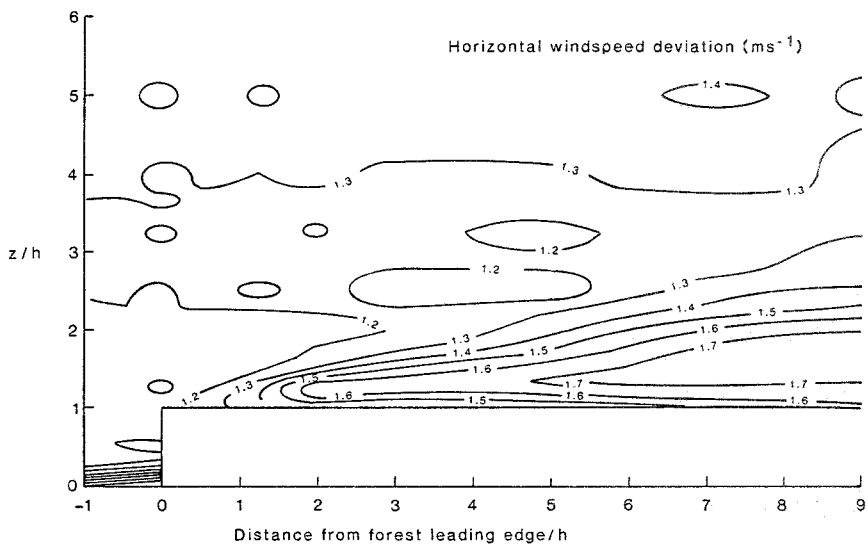

Fig. 11. Contours of velocity standard deviation at forest edge.

in the mean wind suggests shelter, gust loading and sway excitation may not necessarily decrease.

It is expected that at large distances, the flow will approach the mid-forest equilibrium condition. This is not achieved within the limited fetch in the present

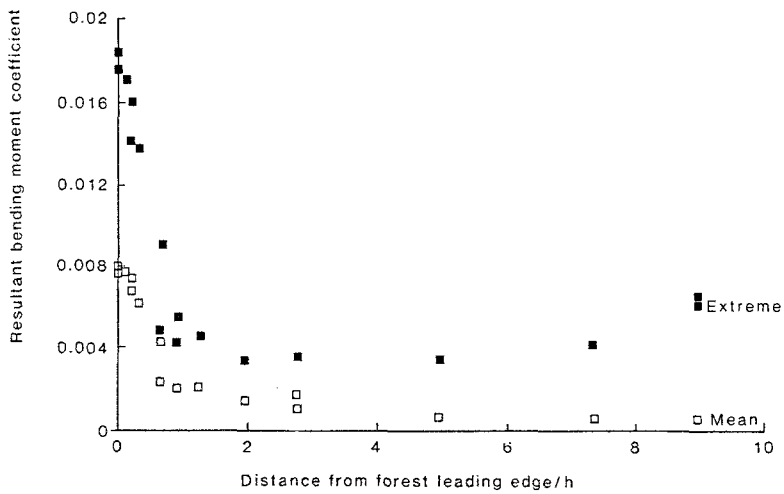

Fig. 12. Change of bending moments with distance back from forest edge.

experiments (Figures 10, 11, 12), but it is clear that the boundary layer will stabilise eventually, with an effective displacement of the ground plane as in Figure 5.

6.2. Bending moments

Figure 12 shows the decay in the bending moments at increasing distances from the upstream plantation edge. As expected, the moments decrease rapidly as the trees become sheltered by upstream rows. Consequently it is to be expected that in a freshly cut edge where the trees have not grown differently, these front rows will be most prone to wind damage.

Both mean and extreme (mode from 10 min full-scale) moments are shown in Figure 12, and it is of interest to observe that the extreme moments show a minimum between two and three tree heights from the edge. In this region, the extremes are unusually close to the mean values, thus suggesting that the impingement of gusts may be inhibited locally, perhaps by the upward flow of displaced air from between the trees. Farther downstream, the extreme moments increase again. Forest management experience indicates that wind damage often occurs at approximately 10 tree heights from a forest edge, and it is a pity that the present model plantation was not sufficiently large to permit an investigation of this point.

7. Forest Clearings

The final investigation in this paper is a set of experiments on the effect of cutting a clearing across a forest. Two-dimensional gaps at right angles to the wind were created by separating the base-panels of the plantation model by up to 1.3m (6.7

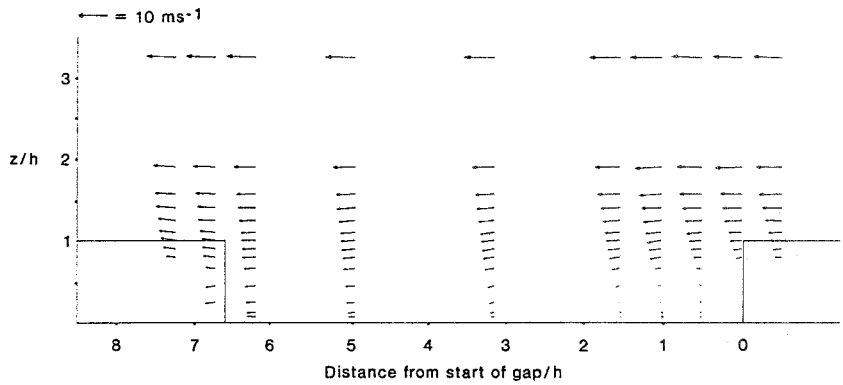

Fig. 13. Wind vectors within a mid-forest clearing.

tree heights). The mid-forest wind simulation was used (Section 2.1), so the gaps were effectively in an infinite forest.

7.1. Wind profiles

Wind speed measurements were made over three gap widths, equivalent to 31, 57 and 100 m full-scale. Figure 13 shows a vector plot of mean velocities in the largest gap. Measured with the laser anemometer, this provides a useful insight into the penetration of the flow into a gap, and also displays the characteristic region of weak recirculating flow in the shelter of the upwind stand.

7.2. Bending moments

Uprooting moments were measured on trees near the sheltered upwind side of each gap. The extreme moments in Figure 14 show that trees in this position experience uprooting moments no different from the mid-forest value (Figure 8). At the exposed downstream side of the gap, the moments are high, but the same rapid development of protective shelter is found within the first few rows, as already noted near a genuine windward forest edge (Figure 12).

Figure 15 focuses attention on the first downstream edge row, and the data for the three gaps is supplemented by the addition of values from square "holes" in the forest canopy. A comparison with Figure 12 reveals the initially surprising fact that the moment coefficients in a gap can be higher than those on a completely exposed windward forest edge. However, this does not mean that the moments themselves are higher, but only that the reference velocity in the denominator of the coefficient (Table II) is lower in mid-forest than at the upstream edge.

The purpose of Figure 15 is to show how sharply the bending moment increases, as soon as even the smallest gap is created within the canopy. A gap of 15 m (one tree height) virtually doubles the moment on the exposed edge. This means that cutting even a narrow access track through a plantation will significantly increase

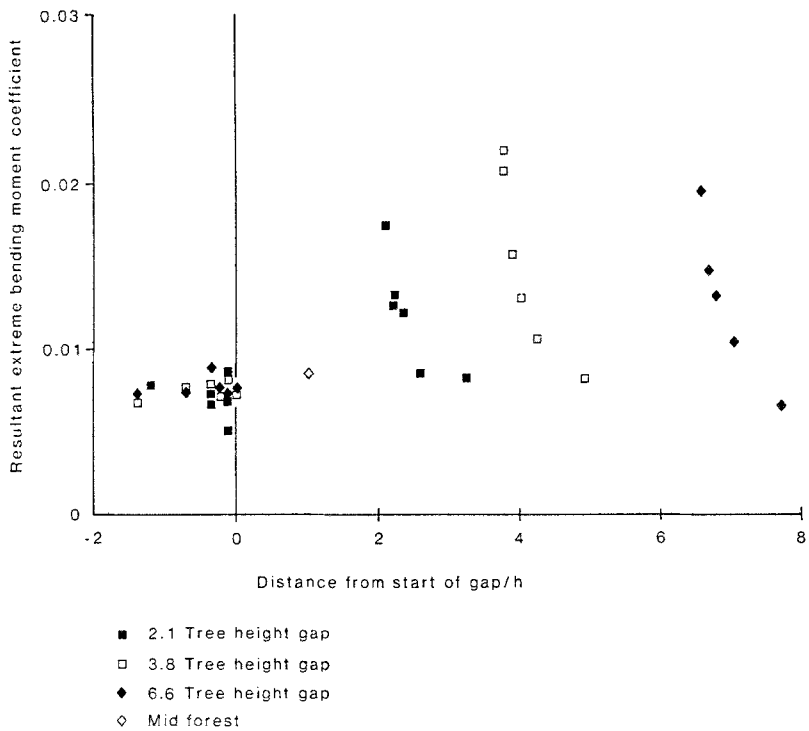

Fig. 14. Bending moments on trees upwind and downwind of mid-forest clearings, compared with fully sheltered mid-forest values.

the risk of wind damage. Interestingly there appears to be little difference in effect between a hole, of the form that often marks the inception of local wind damage, and a gap, which is likely to be man-made.

8. Conclusions

This wind tunnel study has two major points of originality. Firstly, a plantation of aeroelastic tree models has been studied in a correctly modelled turbulent wind with characteristics which agree well with those measured in field trials (Paper 1). Secondly, the uprooting moments on representative models have been measured directly by a sensitive, high-frequency balance, designed and built for the purpose.

From the many results obtained in this programme, those selected for this second paper of the series are those pertaining to a uniform planting density equivalent to 1.73 m spacing. At this density, significant crown-clashing occurs between full-scale trees, but the design of the models was such that crown contact was not realistic. For this reason, absolute values of overturning moments are presented with reservations. In Paper 3, results will be presented for lower planting densities, where crown-clashing is not so important.

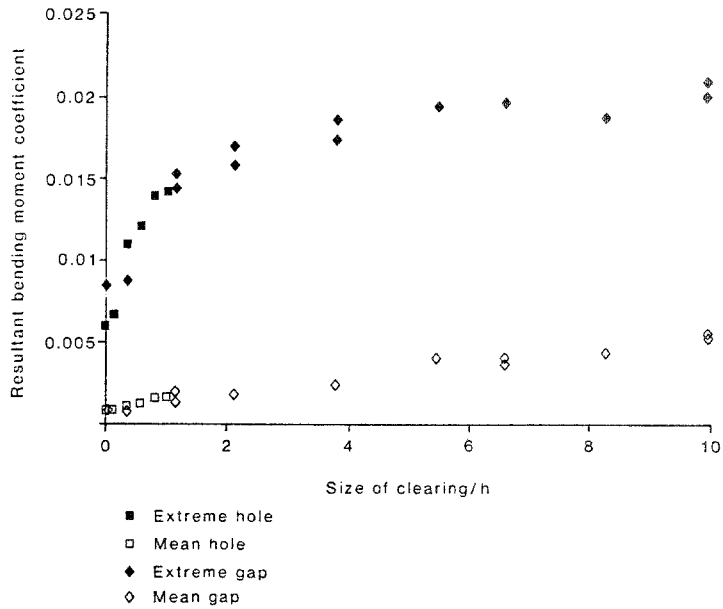

Fig. 15. Bending moments on trees at the downwind edges of mid-forest clearings.

Mid-Forest Results

Although the trees were arrayed in rows, the overturning moments have proved insensitive to wind direction. At the centre of the plantation, moment coefficients based upon tree height and local wind dynamic pressure at 1.9 tree heights, have mean values of order 0.0008 and extreme (10-min mode) values of 0.008. According to the definition in Table II, these mean and extreme coefficient values correspond to actual moments of 1.5 kN m and 15 kN m respectively on a 15m tree in a reference mean wind speed of 30 ms^{-1}. This extreme bending moment is known to be sufficient to overturn some spruce trees of this height on peaty gley soils (Coutts, 1986).

The frequency spectrum of the overturning moments is related to the wind gust spectrum by an admittance function which has the expected characteristics of a classical vibrating system with light to moderate damping. The resonant frequency is a little higher than the peak frequency in the logarithmic wind spectrum and there is evidence to suggest that resonant amplification makes a significant contribution to the magnitude of the extreme overturning moments, primarily through an increased standard deviation.

Effect of Gaps and the Forest Edge

The windward edge of a stand of trees is exposed to higher wind speeds than any other part. Here the maximum overturning moment coefficients are more than

twice the mid-forest values, but the decay in the second, third and subsequent rows is very rapid. This statement relates to measurements on standard mid-forest tree models, and applies therefore, not to naturally grown edge trees with additional live branches, but to those more vulnerable trees which remain after partial harvesting.

An interesting additional observation is that trees from the second to tenth rows experience lower extreme moments than mid-forest trees, probably because the flow near a windward edge includes an up-draught due to the retardation of the initial flow between the trees. This updraught may reduce penetration of the canopy by gusts.

The effect of a cross-wind gap or clearing is similar to that of an upwind edge. The moments downwind of the gap are approximately doubled, even for narrow gaps of no more that two tree heights. Trees on the upwind, sheltered side of clearings remain sheltered.

Accuracy Assessment

Hot wire anemometers are not suitable for measurements in highly turbulent flows, and where appropriate, a laser anemometer has been used instead. In general, instrument errors in the wind tunnel are considered to be small compared with the variability and uncertainty of the quantities being measured. All velocities are random variables, imperfectly simulated in the artificially contrived turbulent wind tunnel flow. Likewise the tree characteristics, particularly the drag coefficient and the mechanical crown-clashing characteristics, lead to uncertainties in the measured bending moments, despite the high sensitivity and accuracy of the balance.

Some of these uncertainties are a consequence of inadequate knowledge of the full scale characteristics being modelled. Others arise from a simple inability to model accurately the characteristics that are known. Where possible, these limitations have been declared, and they should be taken into account when assessing the results of the experiments.

References

Cartwright, D. E. and Longuet-Higgins, M. S.: 1956, 'Statistical Distribution of the Maxima of a Random Function', *Proc. Roy. Soc. A*,**23**, 212.

Coutts, M. P.: 1986, 'Components of Tree Stability in Sitka Spruce on Peaty Gley Soils', *Forestry* **59**, 173–197.

Davenport, A. G.: 1964, 'Note on the Distribution of the Largest Value of a Random Function with Application to Gust Loading', *Proc. Inst. Civil Engrs.* **28**, 187.

ESDU: 1989, *Engineering Sciences Data, Wind Engineering Sub-Series*, Vol. 1, ESDU International plc, 27, Corsham St. London N1 6UA.

Finnigan, J. J. and Mulhearn, P. J.: 1978, 'Modelling Waving Crops in a Wind Tunnel'. *Boundary Layer Meteorol.* **14**, 253–277.

Gardiner, B. A.: 1989, 'Mechanical Characteristics of Sitka Spruce', *Forestry Commission Occasional Paper 24.* ISBN 0 85538 235 X.

Gardiner, B. A.: 1992, 'Mathematical Modelling of the Static and Dynamic Characteristics of Plantation

Trees', in J. Franke and A. Roeder (eds.), *Mathematical Modelling of Forest Ecosystems*, Saulerlanders, Verlag,. Frankfurt am Main, pp. 40–61.

Gardiner, B. A.: 1994, 'Wind and Wind Forces in a Plantation Spruce Forest', Paper 1 of present series, *Boundary-Layer Meteorol.* **67** (in press).

Gardiner, B. A., Stacey, G. R., Belcher, R. E. and Wood, C. J.: 1994, 'Field and Wind Tunnel Assessment of the Implications of Respacing and Thinning on Tree Stability', Paper 3 of present series, Submitted to *Forestry*.

Lieblein J.: 1974, *Efficient Methods of Extreme Value Methodology*, U.S. Nat Bureau of Standards I.R. 75-637.

Lieblein, J.: 1975, *Note on Simplified Estimators for Type* 1 *Extreme Value Distribution*, U.S. Nat. Bureau of Standards I.R. 75-637.

Lo, A. K.: 1990, 'On the Determination of Zero-Plane Displacement and Roughness Length for Flow over Forest Canopies', *Boundary-Layer Meteorol.* **51**, 255–268.

Massey, B. S.: 1983, *Mechanics of Fluids*, (5th Ed.), Van Nostrand Reinhold.

Mayhead, G. J., Gardiner, J. B. H. and Durrant, D. W.: 1975, *Physical Properties of Conifers in Relation to Plantation Stability*. Unpublished Report, Forestry Commission, Edinburgh.

Meroney, R. N.: 1968, 'Characteristics of Wind and Turbulence in and above Model Forests', *J. Appl. Meteorol.* **7**, 780–788.

Papesch, A.: 1984, *Wind and its Effects on (Canterbury) Forests*, PhD. Thesis, University of Canterbury, Christchurch, New Zealand.